JAMA Neurology | Original Investigation

Positron Emission Tomography Imaging With [^{18}F]flortaucipir and Postmortem Assessment of Alzheimer Disease Neuropathologic Changes

Adam S. Fleisher, MD, MAS; Michael J. Pontecorvo, PhD; Michael D. Devous Sr, PhD; Ming Lu, MS, MPH, MD; Anupa K. Arora, MD, MPH; Stephen P. Truocchio, MS; Patricia Aldea, MS; Matthew Flitter, BA; Tricia Locascio, BS; Marybeth Devine, BS; Andrew Siderowf, MD; Thomas G. Beach, MD, PhD; Thomas J. Montine, MD, PhD; Geidy E. Serrano, PhD; Craig Curtis, MD; Allison Perrin, MD; Stephen Salloway, MD, MS; Misty Daniel, CCRC; Charles Wellman, MD; Abhinay D. Joshi, MS; David J. Irwin, MD; Val J. Lowe, MD; William W. Seeley, MD; Milos D. Ikonomovic, MD; Joseph C. Masdeu, MD, PhD; Ian Kennedy, MS; Thomas Harris, MS; Michael Navitsky, MS; Sudeepti Southekal, PhD; Mark A. Mintun, MD; for the A16 Study Investigators

IMPORTANCE Positron emission tomography (PET) may increase the diagnostic accuracy and confirm the underlying neuropathologic changes of Alzheimer disease (AD).

OBJECTIVE To determine the accuracy of antemortem [^{18}F]flortaucipir PET images for predicting the presence of AD-type tau pathology at autopsy.

DESIGN, SETTING, AND PARTICIPANTS This diagnostic study (A16 primary cohort) was conducted from October 2015 to June 2018 at 28 study sites (27 in US sites and 1 in Australia). Individuals with a terminal illness who were older than 50 years and had a projected life expectancy of less than 6 months were enrolled. All participants underwent [^{18}F]flortaucipir PET imaging, and scans were interpreted by 5 independent nuclear medicine physicians or radiologists. Supplemental autopsy [^{18}F]flortaucipir images and pathological samples were also collected from 16 historically collected cases. A second study (FRO1 validation study) was conducted from March 26 to April 26, 2019, in which 5 new readers assessed the original PET images for comparison to autopsy.

MAIN OUTCOMES AND MEASURES [^{18}F]flortaucipir PET images were visually assessed and compared with immunohistochemical tau pathology. An AD tau pattern of flortaucipir retention was assessed for correspondence with a postmortem B3-level (Braak stage V or VI) pathological pattern of tau accumulation and to the presence of amyloid-β plaques sufficient to meet the criteria for high levels of AD neuropathological change. Success was defined as having at least 3 of the 5 readers above the lower bounds of the 95% CI for both sensitivity and specificity of 50% or greater.

RESULTS A total of 156 patients were enrolled in the A16 study and underwent [^{18}F]flortaucipir PET imaging. Of these, 73 died during the study, and valid autopsies were performed for 67 of these patients. Three autopsies were evaluated as test cases and removed from the primary cohort (n = 64). Of the 64 primary cohort patients, 34 (53%) were women and 62 (97%) were white; mean (SD) age was 82.5 (9.6) years; and 49 (77%) had dementia, 1 (2%) had mild cognitive impairment, and 14 (22%) had normal cognition. Prespecified success criteria were met for the A16 primary cohort. The flortaucipir PET scans predicted a B3 level of tau pathology, with sensitivity ranging from 92.3% (95% CI, 79.7%-97.3%) to 100.0% (95% CI, 91.0%-100.0%) and specificity ranging from 52.0% (95% CI, 33.5%-70.0%) to 92.0% (95% CI, 75.0%-97.8%). A high level of AD neuropathological change was predicted with sensitivity of 94.7% (95% CI, 82.7%-98.5%) to 100.0% (95% CI, 90.8%-100.0%) and specificity of 50.0% (95% CI, 32.1%-67.9%) to 92.3% (95% CI, 75.9%-97.9%). The FRO1 validation study also met prespecified success criteria. Addition of the supplemental autopsy data set and 3 test cases, which comprised a total of 82 patients and autopsies for both the A16 and FRO1 studies, resulted in improved specificity and comparable overall accuracy. Among the 156 enrolled participants, 14 (9%) experienced at least 1 treatment-emergent adverse event.

CONCLUSIONS AND RELEVANCE This study's findings suggest that PET imaging with [^{18}F]flortaucipir could be used to identify the density and distribution of AD-type tau pathology and the presence of high levels of AD neuropathological change, supporting a neuropathological diagnosis of AD.

JAMA Neurol. 2020;77(7):829-839. doi:10.1001/jamaneurol.2020.0528
Published online April 27, 2020.

Editorial page 796

Supplemental content

CME Quiz at jamacmelookup.com

Author Affiliations: Author affiliations are listed at the end of this article.

Group Information: The names of the A16 study investigators appear at the end of the article.

Corresponding Author: Adam S. Fleisher, MD, MAS, Avid Radiopharmaceuticals, 3711 Market St, Philadelphia, PA 19104 (afleisher@avidRP.com).

Alzheimer disease (AD) is characterized by aggregated tau-containing neurofibrillary tangles (NFTs)[1] and by amyloid plaque composed largely of aggregated amyloid-β (Aβ) fragments.[2,3] Neuropathological criteria for the diagnosis of AD were established by the National Institute on Aging-Alzheimer Association (NIA-AA)[4] and were updated in 2012 to reflect the current thinking on AD pathological assessment.[5,6] With the advent of biomarkers that enable in vivo identification of underlying AD pathological conditions, and the acceptance that AD begins years before the emergence of cognitive impairment, AD is now commonly accepted as a clinicopathological entity[7,8] that can be diagnosed without histopathological examination, in the presence of appropriate biomarker evidence of an underlying condition.[6,8,9]

Tau is an intracellular protein that binds to and stabilizes axonal microtubules in neurons, thereby regulating intracellular transport.[10] Pathological accumulation of aggregated hyperphosphorylated tau protein in neurons and glia underlies a wide range of neurodegenerative disorders.[11] Compared with cortical Aβ plaque, the density and distribution of phosphorylated tau aggregated in NFTs correlate more closely with AD-associated cognitive impairment and neurodegeneration.[12-14] Thus, an imaging biomarker for pathological tau could potentially aid in the diagnosis and selection of patients for therapy as well as allow for monitoring disease progression and for assessing the response to putative disease-modifying treatments.

Positron emission tomography (PET) ligands have been shown to provide a minimally invasive estimate of the neuropathological features of AD, such as Aβ neuritic plaque deposition.[15-18] Imaging biomarkers for cortical tau have become available.[19,20] Flortaucipir is being developed as a PET tracer for detection of the aggregated tau of AD.[19,21-24] In vitro autoradiography studies of brain tissue from symptomatic patients with AD have found that [18F]flortaucipir signal correlates with the level of paired helical filament tau by immunohistochemistry and binds with a dissociation constant in the approximately 0.5 nM range.[20]

Comparison of tracer binding to aggregated protein in autopsy material is one method of validating a novel PET agent. For example, large autopsy studies have demonstrated a high sensitivity and specificity for amyloid PET to distinguish individuals with subsequent autopsy findings of no or sparse neuritic plaque from individuals with moderate to frequent plaque.[16-18] Studies comparing antemortem tau PET imaging with autopsy have begun assessing the ability of flortaucipir to detect underlying NFTs in AD and non-AD dementias.[25-33] In this case-control diagnostic study, we prospectively evaluated in vivo PET imaging with [18F]flortaucipir in people who had terminal illness with or without dementia to assess the association of tracer pattern and density with established postmortem tau pathological assessment and neuropathological AD criteria.

Key Points

Question Do the findings of visual reads of [18F]flortaucipir positron emission tomography (PET) images correspond with postmortem assessment of Alzheimer disease tau and amyloid pathologies?

Findings In this diagnostic study of 82 individuals with or without dementia, visual reads of [18F]flortaucipir PET scans corresponded with postmortem Braak stages V and VI levels of cortical neurofibrillary tangles and high levels of Alzheimer disease neuropathological change.

Meaning Findings from this study suggest that visual reads of [18F]flortaucipir PET scans may accurately support a pathological diagnosis of Alzheimer disease.

Methods

Study Design

This diagnostic study (18F-AV-1451-A16; NCT02516046), hereafter referred to as A16 primary cohort study), compared PET imaging with [18F]flortaucipir with subsequent postmortem assessment of tau pathology[34] and associated NIA-AA level of Alzheimer disease neuropathologic change (ADNC).[5] The study was approved by the institutional review boards at all study sites, and all participants or authorized representatives signed informed consent before the conduct of study procedures. This study was conducted in compliance with the Declaration of Helsinki[35] and the International Conference on Harmonization Good Clinical Practice guideline.[36]

This multicenter study was conducted from October 2015 through June 2018 by 28 investigators at 28 study sites (27 in the US and 1 in Australia). Five board-certified nuclear medicine physicians or radiologists (eAppendix in the Supplement) independently visually rated flortaucipir PET scans as either having or not having a pattern of flortaucipir retention consistent with AD (**Figure 1**). In a subsequent validation study (18F-AV-1415-FR01; NCT03901092), hereafter referred to as the FR01 validation study, a second set of 5 nuclear medicine physicians or radiologists reinterpreted all available scan data. Both the A16 primary cohort and FR01 validation studies tested the primary hypotheses (1) that an antemortem pattern of [18F]flortaucipir retention consistent with AD would correspond with a postmortem B3-level (Braak stage V or VI) pattern of tau pathology accumulation at autopsy[34] and (2) that the AD pattern would occur selectively in the presence of high amyloid burden, meeting the NIA-AA criteria for high levels of ADNC at autopsy.[5]

Participants

The A16 primary cohort included participants who had terminal illness, were older than 50 years, and had a projected life expectancy of less than 6 months. Cognitive status ranged from clinically normal through dementia, including both AD and non-AD clinical dementia diagnoses. The Informant Questionnaire on Cognitive Decline in the Elderly[37] was administered at baseline. The Mini-Mental State Examination[38] was administered at screening to patients who were capable of testing.

The first 3 participants who had an autopsy were evaluated as test cases and were not included in the primary cohort. Their autopsy results and [18F]flortaucipir scans were used to confirm and assess the adequacy of the planned trial methods.

Figure 1. Positron Emission Tomography With [18F]flortaucipir Visual Read Categories and Comparative Histologic Structure

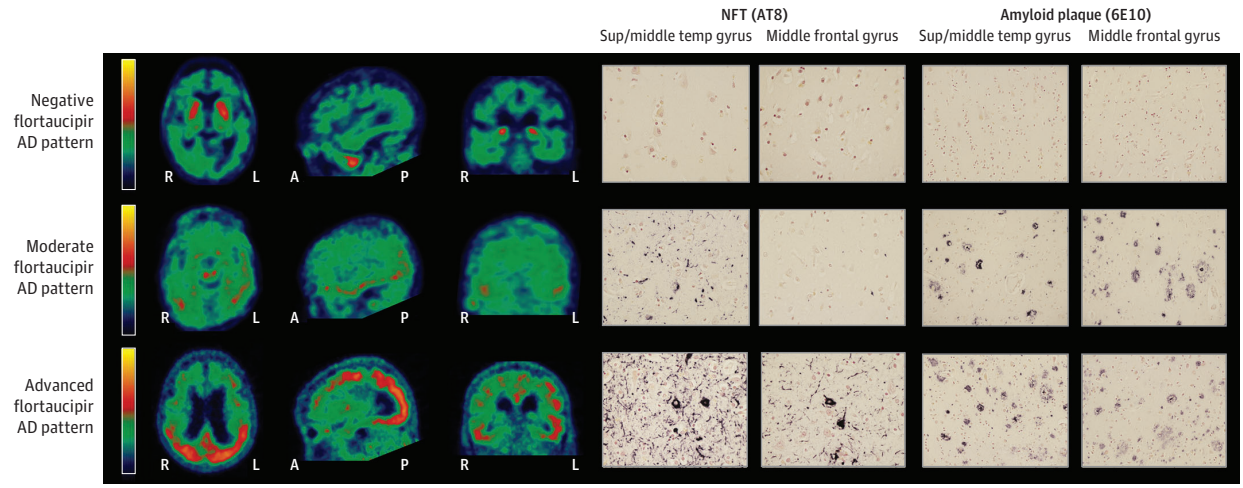

Three cases representing the 3 levels of visual reads and corresponding histologic sections from the superior or middle temporal (sup/middle temp) gyrus (Braak region of interest [ROI] 7) and middle frontal gyrus (Braak ROI 6) stained for neurofibrillary tangles (NFTs) with AT8 antibodies and for amyloid plaque with 6E10 antibodies. Images presented in a blue-green-red-yellow color scale, with cortical counts scaled to 1.65 × the mean cerebellar counts (eAppendix in the Supplement). A indicates anterior; AD, Alzheimer disease; L, left; P, posterior; R, right.

Supplemental Autopsy Cases

Additional images and tissue were collected from academic centers that performed investigator-initiated sponsored [18F]flortaucipir studies (eAppendix in the Supplement). This historically collected data set was added to the A16 study cohort for exploratory analyses. The PET images from these historically collected cases were interpreted by the same 5 readers as those in the A16 primary cohort analysis, and the autopsy tissue was evaluated during a scheduled consensus panel by the same neuropathologists using the same criteria.

PET Imaging Acquisition

Participants underwent 20 minutes of PET imaging (4 × 5-minute acquisition frames) beginning approximately 80 minutes after an intravenous administration of 370 (±10%) MBq of [18F]flortaucipir. Participants with cognitive impairment who did not come to autopsy within 9 months after the flortaucipir scan were either removed from the study or required to undergo a repeat flortaucipir scan for comparison with the neuropathological result. Cognitively normal patients remained eligible for autopsy, regardless of the time from scan to autopsy. Frames were motion-corrected and summed from 80 to 100 minutes after injection. The supplemental autopsy cases also received a target dose of 370 MBq [18F]flortaucipir. Although full dynamic imaging was performed for some participants, the images were processed in the same manner as that used for the primary cohort.

Imaging Visual Interpretation

The flortaucipir PET scans were evaluated by 5 readers who were blinded to clinical and neuropathological results. Scans that were considered unevaluable (eg, head out of field of view, severe motion, acquisition start time offsets, and low counts) by at least 3 of the 5 readers were not used in any analyses. After the prescribed reorientation of the scan, mean counts in the cerebellar region of the brain were estimated. For visualization, a color scale was used that rapidly transitioned between 2 colors. Readers examined specified brain regions (lateral anterior temporal, lateral posterior temporal, occipital, parietal, precuneus, and frontal lobes) and scored each region as negative or positive depending on the presence of an elevated flortaucipir signal of more than 65% above the cerebellar signal (eAppendix in the Supplement).

The flortaucipir PET images were interpreted by visual examination as having regional patterns of tracer uptake that were either not consistent with AD (negative AD tau pattern) or consistent with AD (moderate or advanced AD tau pattern) (Figure 1). A negative AD tau pattern consisted of no increased neocortical activity or increased neocortical activity isolated to the mesial temporal, anterolateral temporal, and/or frontal regions. A moderate AD tau pattern showed increased neocortical activity in the posterolateral temporal or occipital region. An advanced AD tau pattern was defined as increased neocortical activity in the parietal or precuneus region or increased activity in the frontal region accompanied by increases in the posterolateral temporal, parietal, or occipital region.

Interpretation was performed for each hemisphere and for the scan as a whole. In cases in which whole-brain pathological results were not available, the scan classification from the corresponding hemisphere was used for analysis.

Imaging Quantitative Analysis

Scans were motion-corrected by a rigid-body coregistration of all frames to the first frame of that PET session. The motion-corrected series was then corrected for acquisition start time discrepancies and averaged across frames.[24] Because structural imaging was not acquired for the primary cohort,

a PET-to-PET registration method was deployed. First, a flortaucipir template was created in MNI (Montreal Neurological Institute) space from flortaucipir scans registered to the MNI template using the standard PET-to-MRI registration method.[23] Motion-corrected, time-corrected, summed scans were spatially registered to this template using an affine registration. The PERSI (Parametric Estimation of Reference Signal Intensity)[22] algorithm was applied to create a participant-specific white matter reference region. Mean counts from a weighted neocortical target region (multiblock barycentric discriminant analysis; eFigure 1 in the Supplement)[24,39] were extracted and normalized to the mean counts of the reference region to generate standardized uptake value ratios (SUVRs).

Neuropathological Assessment

Neuropathological assessment was performed by 2 authors (T.G.B. and T.J.M.) blinded to clinical and imaging results and using NIA-AA diagnostic scoring guidelines.[5,40] Immunohistochemical staining with the AT8 monoclonal antibody was used as the primary method of Braak pathological staging of NFTs, and the 6E10 $A\beta_{1-42}$ monoclonal antibody was used to detect Aβ plaque. The highest hemisphere NIA-AA pathological scores were compared with the flortaucipir scan visual interpretations. An NFT score of B3, including Braak stages V to VI, was considered positive. Amyloid pathology was evaluated using Thal phase scoring[41] for total amyloid plaque and Consortium to Establish a Registry for Alzheimer Disease (CERAD) scoring[42] for neuritic plaque. The ADNC, consisting of a combination of NFT and amyloid plaque scores, was recorded as not, low, intermediate, or high level per the NIA-AA guidelines.[5,40] A high level of ADNC was considered positive as another standard for comparison with the scans.

Safety Assessment

Treatment-emergent adverse events (TEAE) were defined as adverse events that started or worsened in intensity or frequency on or after [18F]flortaucipir injection and up to 48 hours after injection. TEAEs were classified as either related or not related to [18F]flortaucipir as indicated by the study investigator.

Statistical Analysis

The preplanned A16 primary cohort included all enrolled participants who had valid and evaluable flortaucipir images and who had an autopsy (n = 64), and excluded the 3 test cases and 16 supplemental historically collected autopsy cases. A preplanned exploratory analysis was performed on the full autopsy data set (n = 82), which included the 64 patients in the primary cohort, 2 evaluable autopsies from the 3 test cases, and the 16 supplemental autopsy cases. For both the primary cohort and the full autopsy data set, analyses included assessment of the diagnostic performance (sensitivity and specificity) of the 5 independent readers interpretations of the flortaucipir scans as being consistent with an AD pattern corresponding to an NFT score of B3 and an NIA-AA assignment of high ADNC level. Two-sided 95% CIs, indicating alpha of 0.05 (based on the Wilson score method), of sensitivity and specificity were calculated for each of the 5 readers. Success was defined as having at least 3 of the 5 readers above the lower bounds of the 95% CI for both sensitivity and specificity of 50% or greater. Accuracy, positive predictive value, negative predictive value, and positive and negative likelihood ratios of the flortaucipir imaging classification for each of the 5 readers (relative to NFT and ADNC scores) were also calculated.

In addition, a secondary analysis was performed using the majority read interpretation of PET images from the 5 independent readers. The *majority read* was defined as either a negative, moderate, or advanced flortaucipir AD pattern based on 3 of 5 readers interpreting the PET image in 1 of these 3 read categories. When no majority was reached for 1 of 3 read categories, a majority read was established for either a positive (moderate or advanced) or negative interpretation. If positive, the specific category of positive (moderate or advanced) that had the greater number of read interpretations was used as the majority read. In case of a tie between an advanced and moderate read (eg, advanced=2, moderate=2, negative=1), the moderate read was used as the final interpretation. The majority reads were then compared with NFT scores and ADNC standards for calculation of sensitivity and specificity in a manner identical to the primary analysis. To assess overall inter-reader agreement, Fleiss κ statistics were calculated. The agreement between each pair of readers was assessed for each diagnostic decision using the simple κ coefficient.

Analyses performed on the A16 primary cohort were repeated on the full autopsy data set. Similar analyses were performed for the FR01 validation study. A visual read interpretation for 1 of the 3 test cases was not included in the full autopsy data set analysis because the image was deemed unevaluable by the readers, owing to an inadvertent image processing error. After subsequent motion correction, this image was included for analysis in the FR01 validation study. One supplemental autopsy case was excluded from the FR01 validation data set, with 3 readers declaring the image unevaluable because of low counts. Thus, 82 images were included in the full autopsy data set for both the A16 study and FR01 study, but the data sets differed by 1 case each.

Additional exploratory comparisons were made between quantitative SUVR and the pathological end points for the primary cohort plus the 3 test cases. Receiver operating curves were created to evaluate the ability of the SUVR to identify the pathological end points and the optimal SUVR positivity cut point.

Where applicable, statistical tests were performed with a 2-sided $\alpha = 0.05$. The data analysis for this report was performed using SAS System for Windows, version 9.4 (SAS Institute Inc). All analyses were conducted between August 20, 2018, and September 12, 2019.

Results

Clinical Demographics

A total of 156 participants were enrolled in this diagnostic study, underwent flortaucipir imaging, and were included in a safety assessment (**Table 1**). Before study completion, 73 partici-

Table 1. Demographic Characteristics of A16 Original Eligible Cohort, Primary Cohort, Test Cases, and Supplemental Autopsy Cases

Variable	Mean (SD)			
	Normal cognition	Mild cognitive impairment	Dementia	Total
Original eligible cohort				
No.	50	3	103	156
Age, y	75.2 (15.1)	82.0 (10.4)	82.5 (10.5)	80.2 (12.5)
Female sex, No. (%)	23 (46)	1 (33)	62 (60)	86 (55)
White race/ethnicity, No. (%)	42 (84)	3 (100)	98 (95)	143 (92)
Educational level, y	14.4 (3.16)	11.3 (5.03)	14.9 (3.25)	14.7 (3.27)
MMSE score[a]	27.3 (3.44)	23 (2.65)	11.8 (9.47)	21.3 (9.83)
IQCODE score[a]	3.2 (0.53)	3.5 (0.40)	4.8 (0.39)	4.5 (0.78)
Primary cohort				
No. (%)	14 (22)	1 (2)	49 (77)	64 (100)
Age, y	78.6 (12.1)	76	83.8 (8.6)	82.5 (9.6)
Female sex, No. (%)	6 (43)	0	28 (57)	34 (53)
White race/ethnicity, No. (%)	14 (100)	1 (100)	47 (96)	62 (97)
Educational level, y	14.9 (2.91)	16	15.1 (3.53)	15.0 (3.36)
MMSE score[b]	26.2 (4.21)	26	6.9 (6.86)	18 (11.07)
IQCODE score[b]	3 (0.60)	3.4	4.9 (0.31)	4.5 (0.83)
Test cases				
No.	0	0	3	3
Age, y	NA	NA	84.0 (5.2)	84.0 (5.2)
Female sex, No. (%)	NA	NA	1 (33)	1 (33)
White race/ethnicity, No. (%)	NA	NA	3 (100)	3 (100)
Educational level, y	NA	NA	16.0 (4.00)	16.0 (4.00)
MMSE score[c]	NA	NA	20	20
IQCODE score[c]	NA	NA	4.9 (0.14)	4.9 (0.14)
Supplemental autopsy cases				
No.	4	3	9	16
Age, y	86.8 (12.7)	72.3 (8.9)	75.4 (9.9)	77.7 (11.2)
Female sex, No. (%)	2 (50)	0	4 (44)	6 (38)
White race/ethnicity, No. (%)	4 (100)	3 (100)	9 (100)	16 (100)
Educational level, y	15.3 (4.57)	16 (0)	15.1 (3.33)	15.3 (3.20)

Abbreviations: IQCODE, Informant Questionnaire on Cognitive Decline in the Elderly; MMSE, Mini-Mental State Examination; NA, not applicable.

[a] MMSE sample size = 85; IQCODE sample size = 132.

[b] MMSE sample size = 26; IQCODE sample size = 59.

[c] MMSE sample size = 1; IQCODE sample size = 3.

pants died within 9 months of imaging, of whom 67 (92%) had a valid study autopsy (eFigure 2 in the Supplement). After removal of the 3 test cases, the remaining 64 participants were included in the A16 primary cohort, with autopsy occurring a mean (SD) 16.2 (15.0) hours from the recorded time of death and 2.6 (2.14) months after [18F]flortaucipir imaging.

Of the 64 patients in the primary cohort, 34 (53%) were women, 62 (97%) were white, and the mean (SD) age was 82.5 (9.6) years (Table 1). Of the 64 primary cohort patients, 49 (77%) had dementia, 1 (2%) had mild cognitive impairment, and 14 (22%) had normal cognition. Of the 49 patients with dementia, 33 had a clinical diagnosis of AD based on medical history and 16 had non-AD clinical diagnosis at baseline (eTable 1 in the Supplement).

All 3 test-case patients had a clinical dementia syndrome, 2 had an AD diagnosis, and 1 had an undetermined diagnosis. The supplemental autopsy cases (n = 16) had a mean (SD) reported age of 77.7 (11.2) years, comprised 6 women (37.5%), and all were white individuals. Four had normal cognition, 3 had non-AD mild cognitive impairment, 2 had AD dementia, and 7 had non-AD dementia (Table 1; eTable 1 in the Supplement).

Safety Assessment

Among the 156 enrolled participants, 14 (9%) experienced at least 1 treatment-emergent adverse event (eTable 2 in the Supplement). Agitation (n = 3) and headache (n = 2) were the most common of these events. Three participants (2%) experienced serious adverse events within 48 hours of the flortaucipir scan: death from acute kidney failure, death from malignant neoplasm, and nonfatal myocardial infarction during hemodialysis. Both death events were reported by the investigator as severe adverse events that were not associated with the study drug or procedure.

Primary Cohort Outcomes

The A16 primary cohort analysis of 64 patients met prespecified success criteria, with flortaucipir PET imaging demonstrating statistically significant sensitivity and specificity for detecting both NFT score of B3 and high level of ADNC, as de-

Table 2. Diagnostic Performance of 5 Independent Reader Interpretations of the [18F]flortaucipir Images in the A16 Primary Cohort and the Full Autopsy Data Set Cohort[a]

Reader No./Cohort	TP	FN	FP	TN	% (95% CI) Sensitivity	Specificity	Accuracy (95% CI)	NPV (95% CI)	PPV (95% CI)
Flortaucipir PET read compared with B3 NFT score									
1									
PC[b]	38	1	8	17	97.4 (86.8-99.5)	68.0 (48.4-82.8)	85.9 (75.4-92.4)	94.4 (74.2-99.0)	82.6 (69.3-90.9)
FAS[c]	43	3	8	28	93.5 (82.5-97.8)	77.8 (61.9-88.3)	86.6 (77.6-92.3)	90.3 (75.1-96.7)	84.3 (72.0-91.8)
2									
PC	36	3	2	23	92.3 (79.7-97.3)	92.0 (75.0-97.8)	92.2 (83.0-96.6)	88.5 (71.0-96.0)	94.7 (82.7-98.5)
FAS	41	5	2	34	89.1 (77.0-95.3)	94.4 (81.9-98.5)	91.5 (83.4-95.8)	87.2 (73.3-94.4)	95.3 (84.5-98.7)
3									
PC	36	3	3	22	92.3 (79.7-97.3)	88.0 (70.0-95.8)	90.6 (81.0-95.6)	88.0 (70.0-95.8)	92.3 (79.7-97.3)
FAS	41	5	3	33	89.1 (77.0-95.3)	91.7 (78.2-97.1)	90.2 (81.9-95.0)	86.8 (72.7-94.2)	93.2 (81.8-97.7)
4									
PC	36	3	6	19	92.3 (79.7-97.3)	76.0 (56.6-88.5)	85.9 (75.4-92.4)	86.4 (66.7-95.3)	85.7 (72.2-93.3)
FAS	41	5	6	30	89.1 (77.0-95.3)	83.3 (68.1-92.1)	86.6 (77.6-92.3)	85.7 (70.6-93.7)	87.2 (74.8-94.0)
5									
PC	39	0	12	13	100.0 (91.0-100.0)	52.0 (33.5-70.0)	81.3 (70.0-88.9)	100.0 (77.2-100.0)	76.5 (63.2-86.0)
FAS	42	4	12	24	91.3 (79.7-96.6)	66.7 (50.3-79.8)	80.5 (70.6-87.6)	85.7 (68.5-94.3)	77.8 (65.1-86.8)
Majority reads									
PC	36	3	5	20	92.3 (79.7-97.3)	80.0 (60.9-91.1)	87.5 (77.2-93.5)	87.0 (67.9-95.5)	87.8 (74.5-94.7)
FAS	41	5	5	31	89.1 (77.0-95.3)	86.1 (71.3-93.9)	87.8 (79.0-93.2)	86.1 (71.3-93.9)	89.1 (77.0-95.3)
Flortaucipir PET read compared with high ADNC score									
1									
PC	37	1	9	17	97.4 (86.5-99.5)	65.4 (46.2-80.6)	84.4 (73.6-91.3)	94.4 (74.2-99.0)	80.4 (66.8-89.3)
FAS	40	1	11	30	97.6 (87.4-99.6)	73.2 (58.1-84.3)	85.4 (76.1-91.4)	96.8 (83.8-99.4)	78.4 (65.4-87.5)
2									
PC	36	2	2	24	94.7 (82.7-98.5)	92.3 (75.9-97.9)	93.8 (85.0-97.5)	92.3 (75.9-97.9)	94.7 (82.7-98.5)
FAS	39	2	4	37	95.1 (83.9-98.7)	90.2 (77.5-96.1)	92.7 (84.9-96.6)	94.9 (83.1-98.6)	90.7 (78.4-96.3)
3									
PC	36	2	3	23	94.7 (82.7-98.5)	88.5 (71.0-96.0)	92.2 (83.0-96.6)	92.0 (75.0-97.8)	92.3 (79.7-97.3)
FAS	39	2	5	36	95.1 (83.9-98.7)	87.8 (74.5-94.7)	91.5 (83.4-95.8)	94.7 (82.7-98.5)	88.6 (76.0-95.0)
4									
PC	36	2	6	20	94.7 (82.7-98.5)	76.9 (57.9-89.0)	87.5 (77.2-93.5)	90.9 (72.2-97.5)	85.7 (72.2-93.3)
FAS	39	2	8	33	95.1 (83.9-98.7)	80.5 (66.0-89.8)	87.8 (79.0-93.2)	94.3 (81.4-98.4)	83.0 (69.9-91.1)
5									
PC	38	0	13	13	100.0 (90.8-100.0)	50.0 (32.1-67.9)	79.7 (68.3-87.7)	100.0 (77.2-100.0)	74.5 (61.1-84.5)
FAS	40	1	14	27	97.6 (87.4-99.6)	65.9 (50.5-78.4)	81.7 (72.0-88.6)	96.4 (82.3-99.4)	74.1 (61.1-83.9)
Majority reads									
PC	36	2	5	21	94.7 (82.7-98.5)	80.8 (62.1-91.5)	89.1 (79.1-94.6)	91.3 (73.2-97.6)	87.8 (74.5-94.7)
FAS	39	2	7	34	95.1 (83.9-98.7)	82.9 (68.7-91.5)	89.0 (80.4-94.1)	94.4 (81.9-98.5)	84.8 (71.8-92.4)

Abbreviations: ADNC, Alzheimer disease neuropathologic change; FAS, full autopsy data set; FN, false negative; FP, false positive; NFT, neurofibrillary tangles; NPV, negative predictive value; PC, primary cohort; PET, positron emission tomography; PPV, positive predictive value; TN, true negative; TP, true positive.

[a] Sample size and accuracy statistics comparing [18F]flortaucipir PET visual reads for all 5 individual readers compared with pathological findings for identifying B3 NFT scores and high ADNC scores.

[b] Primary cohort included 64 participants.

[c] Full autopsy data set included 82 cases.

termined by the interpretations of at least 3 of the 5 physican readers of the PET scans (**Table 2**; **Figure 2**). For the B3 level, sensitivity ranged from 92.3% (95% CI, 79.7%-97.3%) to 100.0% (95% CI, 91.0%-100.0%), and specificity ranged from 52.0% (95% CI, 33.5%-70.0%) to 92.0% (95% CI, 75.0%-97.8%). For the high ADNC level, sensitivity was 94.7% (95% CI, 82.7%-98.5%) to 100.0% (95% CI, 90.8%-100.0%) and specificity was 50.0% (95% CI, 32.1%-67.9%) to 92.3% (95% CI, 75.9%-97.9%) (Table 2). The majority read analysis for the A16 primary cohort showed similar results for B3 level sensitivity

Figure 2. Braak Neurofibrillary Tangle (NFT) Scores vs Majority Read Interpretations for the A16 Primary Cohort (n = 64)

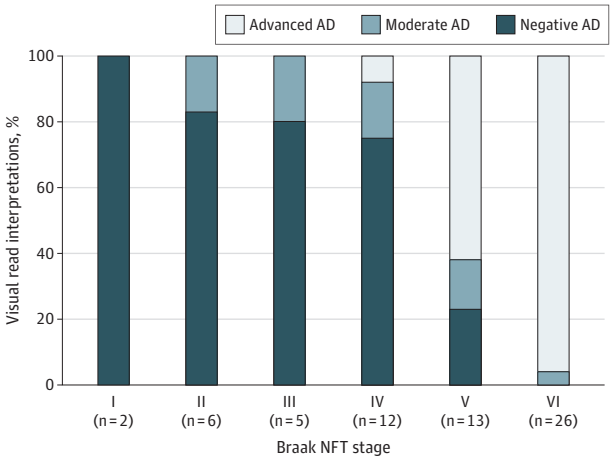

AD, Alzheimer disease; Advanced AD, consistent with advanced AD tau pattern; Moderate AD, consistent with moderate AD tau pattern; and Negative AD, not consistent with AD tau pattern.

Figure 3. Consortium to Establish a Registry for Alzheimer Disease (CERAD) Amyloid Plaque Scores vs Braak Neurofibrillary Tangle (NFT) Scores

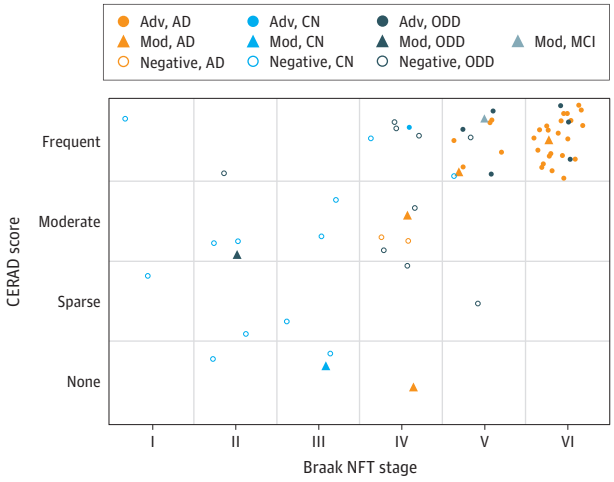

A16 primary cohort. CERAD amyloid plaque scores vs Braak NFT stages (highest score from both hemispheres), categorized by clinical diagnosis and flortaucipir majority visual read category. Data points were randomly scattered within each grid square to minimize overlap for presentation purposes. AD, Alzheimer disease; Adv, consistent with advanced AD tau pattern; CN, cognitively normal; MCI, mild cognitive impairment; Mod, consistent with moderate AD tau pattern; Negative, not consistent with AD tau pattern; and ODD, other non-AD dementia diagnoses. All PET image reads represent the majority read interpretation for each image.

(92.3%; 95% CI, 79.7%-97.3%) and specificity (80.0%; 95% CI, 60.9%-91.1%), and for high ADNC level sensitivity (94.7%; 95% CI, 82.7%-98.5%) and specificity (80.8%; 95% CI, 62.1%-91.5%) (Table 2).

For the full autopsy data set (n = 82), all 5 readers met success criteria with lower confidence limits of sensitivity and specificity greater than 50% for the NFT score of B3 with sensitivity ranging from 89.1% (95% CI, 77.0%-95.3%) to 93.5% (95% CI, 82.5%-97.8%) and specificity ranging from 66.7% (95% CI, 50.3%-79.8%) to 94.4% (95% CI, 81.9%-98.5%). Success criteria were also met for high level of ADNC with sensitivity ranging from 95.1% (95% CI, 83.9%-98.7%) to 97.6% (95% CI 87.4%-99.6%) and specificity ranging from 65.9% (95% CI, 50.5%-78.4%) to 90.2% (95% CI, 77.5%-96.1%) (Table 2). The majority read analysis for the A16 full autopsy data set showed similar results for B3 level sensitivity (89.1%; 95% CI, 77.0%-95.3%) and specificity (86.1%; 95% CI, 71.3%-93.9%), and for high ADNC level sensitivity (95.1%; 95% CI, 83.9%-98.7%) and specificity (82.9%; 95% CI, 68.7%-91.5%) (Table 2).

In the full autopsy data set, there were 26 impaired participants with a non-AD clinical diagnosis. Of these, 19 had less than high levels of ADNC at autopsy. In 16 of these 19 participants, the flortaucipir PET images were accurately interpreted as not being consistent with an AD pattern (eTable 1 in the Supplement).

The FR01 validation study also met the prespecified success criteria for both the FR01 primary cohort (n = 64) and full autopsy data set (n = 82) analyses, demonstrating statistically significant sensitivity and specificity (above 95% CI lower limits >50%) of flortaucipir PET imaging for detecting both the NFT score of B3 NFT and high ADNC level by at least 3 of the 5 readers. Similar sensitivity and specificity results were seen for the majority read analyses (eTable 3 in the Supplement).

Interrater reliability in both the A16 primary cohort and FR01 validation studies was high. For the A16 study, all read scans (n = 105 of enrolled patients) showed 89.9% agreement (Fleiss κ, 0.80; $P < .001$); the primary cohort scans (n = 64) showed 88.4% agreement (Fleiss κ, 0.74; $P < .001$). In the FR01 study (n = 82), the Fleiss κ value was 0.82 ($P < .001$).

Pathological cases covered a full range of tau pathology from Braak stages I to VI NFTs (Figure 2, **Figure 3**, and eFigure 3 in the Supplement). Specifically, 46 (56%) of the full autopsy data set cases were classified as having an NFT score of B3, and 42 (91%) of these cases had amyloid neuritic plaque with moderate or frequent CERAD scores. Only 2 of these cases with an NFT score of B3 and moderate to frequent CERAD scores had normal cognition; 8 of 23 (35%) of cases with B2 NFT scores were amyloid negative (CERAD none-sparse score), and 3 of those 8 had normal cognition. Of the 46 cases with an AD pattern on flortaucipir scan (by majority 3 of 5 readers), 43 (94%) had amyloid plaque with moderate to frequent CERAD scores.

For quantitative analysis, 60 (90%) of 67 scans (primary cohort plus test cases) met the scan quality criteria for SUVR calculation; 6 scans (9%) had severe inter- and within-frame motion, and 1 scan (2%) was acquired outside of the allowable postinjection acquisition time window. Receiver operator curve assessment established an optimal SUVR cut point greater than 1.113 for defining a positive scan. This quantitative cut point yielded a sensitivity of 84.2% for an NFT score of B3 and 86.5% for a high level of ADNC, with 100% specificity for both autopsy measures (eFigure 3 in the Supplement).

Discussion

The A16 study demonstrated statistically significant sensitivity and specificity of PET imaging with [18F]flortaucipir for detecting tau neurofibrillary pathology (NFT score of B3 corresponding with Braak stages V and VI) and high levels of ADNC neuropathologic changes (according to NIA-AA criteria). These results were confirmed by a second set of independent physician readers of the PET scans in the FR01 validation study. The primary study results were further strengthened in secondary exploratory analyses that included 16 supplemental autopsy cases, establishing a high specificity for detecting AD tau. A high degree of interrater reliability was observed. Administration of flortaucipir F18 was safe with relatively few adverse effects among patients enrolled in the A16 study, many of which were common events among older adults, people with dementia, and people with terminal illness.

Amyloid and tau pathologies may begin independently[6,43] but are highly associated with each other in symptomatic stages of AD.[44] In this study, the presence of high levels of AD-type NFTs, as assessed by an AD pattern on a PET scan with [18F]flortaucipir, was accompanied by a probability of moderate to frequent neuritic plaque present at autopsy. These results are consistent with previously observed correspondence between elevated flortaucipir PET signal and elevated signal on amyloid PET.[23,45] These findings support the potential for PET imaging with [18F]flortaucipir to assist in the diagnosis of AD as defined by the NIA-AA research framework.[6]

An AD pattern, as defined in this study, required evidence of [18F]flortaucipir uptake beyond the mesial and anterior lateral temporal lobes. For visual reads of PET scans, the mesial temporal regions can be challenging to interpret owing to the potential bleed-in from off-target binding in the choroid plexus and atrophy-associated partial-volume effects. Furthermore, although these areas are key in early NFT accumulation in AD, isolated tau in these regions can represent B1-level NFTs, which are associated with not or low levels of ADNC.[5] In addition, mesial temporal lobe NFTs in the absence of substantial Aβ or neuritic plaque can occur in older individuals without cognitive impairment, those with mild impairment, or those with cognitive impairment associated with other causes than AD. This consequence can pose a diagnostic dilemma and suggest comorbid pathological conditions distinct from AD.[46,47] Therefore, including these regions in a diagnostic criterion for an AD pattern on flortaucipir PET images may reduce the specificity of AD neuropathological diagnosis.

The NFT levels below B3 are not as strongly associated with cognitive impairment or moderate to frequent neuritic amyloid plaque burden. Although the presence of B3 score may predict the presence of substantial amyloid plaque, amyloid plaque is often present in the absence of B3-level NFTs, particularly in earlier stages of AD.[6,48,49] Similarly, approximately 20% (19%-23%) of participants with positive amyloid PET scans have no or low levels of [18F]flortaucipir binding by quantitative or visual interpretation.[21,23,50-52] Analyses from the National Alzheimer Coordinating Center pathological database have indicated that individuals with a B2 score had clinically normal result at a rate of 25.3% (34 of 134), and 41 (37.6%) of 109 people with Aβ at autopsy had a B2 score.[5] As such, an AD pattern on a flortaucipir PET scan, as defined here, and the presence of B3-level NFTs is associated with the presence of both key AD pathologies. However, a pattern not consistent with AD on flortaucipir PET scan (which may include isolated uptake in the mesial, anterior lateral temporal, or frontal lobes) would not rule out the presence of AD-associated amyloid pathology or lower levels of NFT pathology.

Exploratory analysis using quantitation to identify positive or negative flortaucipir PET scans similarly resulted in the high accuracy of detecting the standard for both NFTs and NIA-AA neuropathological AD diagnosis. Our previously published report of the 3 test cases in the A16 study demonstrated regional relationships between quantitative flortaucipir PET signal and neocortical phosphorylated paired helical filament tau concentrations (Pearson $r = 0.81$; $P < .001$).[53] In support of this finding and the quantitative data presented herein, a recent study of 26 cases comparing flortaucipir PET image and autopsy findings demonstrated a sensitivity of 87% and specificity of 82% for identifying AD-spectrum pathological diagnoses, using quantitative analysis of a mesial, inferior, or middle temporal lobe region of interest.[25] Twelve of these autopsy-confirmed cases had pathological evidence of Braak stages IV to VI NFTs (2 cases with Braak stage IV) with moderate to frequent neuritic plaques and were above the SUVR threshold for positivity for the [18F]flortaucipir temporal lobe region of interest. Together, these results suggest the potential use of quantitative analysis to support visual read interpretation of flortaucipir F18 scan images. Further method improvements, including quantitative analysis of mesial temporal structures,[25,54,55] may alter the sensitivity of [18F]flortaucipir to detect earlier pathological stages of NFTs.

[18F]flortaucipir appears to bind poorly to non-AD tau pathologies such as those seen in frontotemporal dementias, progressive supranuclear palsy, corticobasal degeneration, and chronic traumatic encephalopathy.[27,30,32,50,56,57] Cortical [18F]flortaucipir PET signal in patients with non-AD dementias is generally lower than expected than that seen in typical patients with AD and, when present, tends to be greatest in anterior temporal lobes, frontal lobe and striatum/globus pallidus, and in some reports of white matter foci.[27,28,30-32] A multinational flortaucipir F18 imaging study that evaluated 719 participants with clinical diagnoses of AD dementia, non-AD neurodegenerative disorders, and mild cognitive impairment as well as controls with normal cognition demonstrated a high level of discriminative accuracy of [18F]flortaucipir for AD compared with other neurocognitive disorders.[50] In the full autopsy data set presented herein, 16 of 19 cases with less than high levels of ADNC at autopsy had flortaucipir PET images interpreted as not consistent with an AD pattern. Overall, these non-AD clinical diagnosis cases support the high specificity of PET imaging with [18F]flortaucipir for distinguishing AD from non-AD tau pathologies. However, larger sample sizes are needed to confirm this finding.

Limitations

This study has several limitations. The A16 study cohort was older than the typical symptomatic patients with AD recruited into clinical trials, had more advanced clinical disease with only 1 case of mild cognitive impairment, and lacked racial/ethnic diversity. These characteristics may have implications for the visual and quantitative interpretation of PET scans and for the associations with underlying pathological features. In addition, the visual interpretations of PET scans used in this study showed the best accuracy for detecting the most advanced stages of NFT tau load and distribution as well as ADNC. Earlier stages of AD may meet intermediate pathological diagnostic criteria or have neuritic plaque with moderate or frequent CERAD scores in the absence of substantial tau.[6] In addition, up to 2 of the 5 readers did not meet the statistical accuracy criteria for specificity for the primary outcomes of the A16 primary outcome and FR01 validation studies. This finding was largely associated with overcalling small, noncontiguous foci of activity in the temporal lobes, resulting in a false-positive AD pattern read. This level of activity may represent noise or early spread of tau. PET scan read errors may also have been associated with imprecise drawing of the cerebellar reference region, resulting in reduced mean cerebellar counts and relatively increased cortical signal above the threshold. These types of scan read errors are potentially mitigated through improved reader training or procedural automation. Although [18F]flortaucipir retention in the neocortex appeared to match the distribution of aggregated tau in AD at autopsy, [18F]flortaucipir retention in subcortical structures also appeared to represent off-target binding. The source of this binding is unknown, but given these locations, it can typically be distinguished from neocortical binding in regions associated with AD pathology.

Conclusions

Results of this study support the hypothesis that, with a high sensitivity and moderate to high specificity, PET imaging with [18F]flortaucipir is able to identify the underlying presence of NFTs at the B3 level and a high level of ADNC per the NIA-AA criteria, consistent with a neuropathological diagnosis of AD.[5] In appropriate clinical cases of adults who have undergone adequate neurological assessment and have been evaluated for AD or other causes of cognitive decline, PET imaging with [18F]flortaucipir may help in establishing a diagnosis of AD. Further research is required into the potential value of [18F]flortaucipir imaging in earlier clinicopathological stages of disease.

ARTICLE INFORMATION

Accepted for Publication: January 10, 2020.

Published Online: April 27, 2020. doi:10.1001/jamaneurol.2020.0528

Author Affiliations: Avid Radiopharmaceuticals, Philadelphia, Pennsylvania (Fleisher, Pontecorvo, Devous, Lu, Arora, Truocchio, Aldea, Flitter, Locascio, Devine, Kennedy, Harris, Navitsky, Southekal, Mintun); University of Pennsylvania, Philadelphia (Siderowf, Irwin); Banner Sun Health Research Institute, Sun City, Arizona (Beach, Serrano); Stanford University, Stanford, California (Montine); Waypoint Research, Windermere, Florida (Curtis); Banner Alzheimer's Institute, Phoenix, Arizona (Perrin); Butler Hospital, Providence, Rhode Island (Salloway); Pacific Research Network, San Diego, California (Daniel); Hospice of the Western Reserve, Cleveland, Ohio (Wellman); Imaginab, Inglewood, California (Joshi); Mayo Clinic, Rochester, Minnesota (Lowe); University of California, San Francisco, San Francisco (Seeley); University of Pittsburgh, Pittsburgh (Ikonomovic); Houston Methodist Institute for Academic Medicine, Houston, Texas (Masdeu).

Author Contributions: Dr Fleisher had full access to all of the data in the study and takes responsibility for the integrity of the data and the accuracy of the data analysis.
Concept and design: Fleisher, Pontecorvo, Devous, Lu, Truocchio, Flitter, Siderowf, Beach, Seeley, Masdeu, Mintun.
Acquisition, analysis, or interpretation of data: Fleisher, Devous, Lu, Arora, Truocchio, Aldea, Flitter, Locascio, Devine, Siderowf, Beach, Montine, Serrano, Curtis, Perrin, Salloway, Daniel, Wellman, Joshi, Irwin, Lowe, Seeley, Ikonomovic, Masdeu, Kennedy, Harris, Navitsky, Southekal, Mintun.
Drafting of the manuscript: Fleisher, Pontecorvo, Devous, Lu, Aldea, Flitter, Salloway, Southekal.
Critical revision of the manuscript for important intellectual content: Fleisher, Pontecorvo, Devous, Lu, Arora, Truocchio, Aldea, Locascio, Devine, Siderowf, Beach, Montine, Serrano, Curtis, Perrin, Daniel, Wellman, Joshi, Irwin, Lowe, Seeley, Ikonomovic, Masdeu, Kennedy, Harris, Navitsky, Southekal, Mintun.
Statistical analysis: Lu.
Obtained funding: Lowe, Seeley, Ikonomovic, Mintun.
Administrative, technical, or material support: Fleisher, Pontecorvo, Arora, Truocchio, Aldea, Flitter, Locascio, Devine, Beach, Curtis, Perrin, Salloway, Daniel, Lowe, Ikonomovic, Masdeu, Harris, Navitsky, Southekal, Mintun.
Supervision: Fleisher, Pontecorvo, Devous, Aldea, Flitter, Devine, Siderowf, Beach, Montine, Seeley, Mintun.
Other—image analysis, data analysis: Joshi.
Other—Flortuacipir processing and analysis: Kennedy.

Conflict of Interest Disclosures: Dr Fleisher reported being a full-time employee of Avid Radiopharmaceuticals and being a minor shareholder in Eli Lilly and Company. Dr Pontecorvo reported receiving other from Eli Lilly and Company and being a full-time employee of Avid Radiopharmaceuticals during the conduct of the study. Dr Devous reported being a full-time employee of Avid Radiopharmaceuticals during the conduct of the study. Dr Lu reported being a full-time employee of Avid Radiopharmaceuticals during the conduct of the study. Dr Arora reported being a full-time employee of Avid Radiopharmaceuticals during the conduct of the study. Mr Truocchio reported being a full-time employee of Avid Radiopharmaceuticals during the conduct of the study. Ms Aldea reported receiving other from Eli Lilly and Company during the conduct of the study. Mr Flitter reported receiving other from Eli Lilly and Company during the conduct of the study and being a full-time employee of Avid Radiopharmaceuticals. Ms Devine reported being a full-time employee of Avid Radiopharmaceuticals during the conduct of the study. Dr Siderowf reported receiving personal fees from Avid Radiopharmaceuticals during the conduct of the study and being a former employee of Avid Radiopharmaceuticals. Dr Beach reported receiving grants from Avid Radiopharmaceuticals during the conduct of the study and personal fees from Vivid Genomics and Prothena Biosciences, and holding stock options with Vivid Genomics. Dr Montine reported receiving personal fees and consulting fees from Avid Radiopharmaceuticals during the conduct of the study. Dr Serrano reported being a full-time employee of Avid Radiopharmaceuticals during the conduct of the study. Dr Perrin reported receiving other from Banner Alzheimer's Institute during the conduct of the study. Mr Joshi reported being a former employee of Avid Radiopharmaceuticals. Dr Irwin reported receiving grants from the National Institutes of Health (NIH) and from Avid Radiopharmaceuticals during the conduct of the study. Dr Lowe reported receiving nonfinancial support from Avid Radiopharmaceuticals, grants from GE Healthcare, and grants from Seimens Molecular Imaging outside the submitted work. Dr Ikonomovic reported receiving grants from the NIH during the conduct of the study. Dr Masdeu reported receiving grants from Eli Lilly and Company during the conduct of the study as well as grants and personal fees from GE Healthcare outside the submitted work. Mr Kennedy reported being a full-time employee of Avid Radiopharmaceuticals during the conduct of the study. Mr Harris reported being a full-time

employee of Avid Radiopharmaceuticals during the conduct of the study. Dr Southekal reported being a full-time employee of Avid Radiopharmaceuticals during the conduct of the study and being an employee of and minor stockholder in Eli Lilly and Company. Dr Mintun reported being an employee of Eli Lilly and Company. No other disclosures were reported.

Funding/Support: This study and the confirmatory reader study were funded by Avid Radiopharmaceuticals, a wholly owned subsidiary of Eli Lilly and Company, which owns a license to the patent of [18F]flortaucipir. The supplemental autopsy cases data were provided by the following academic collaborators with independently funded preexisting autopsy and imaging data: Drs Irwin and (Murray) Grossman (funded by NIH grants AG017586 and NIH AG054519); Dr Lowe (funded by NIH grants P50 AG016574, R01 NS89757, R01 NS089544, R01 DC10367, R01 AG011378, R01 AG041851, R01 AG034676, R01 AG054449, R01 NS097495, U01 AG006786, and R21 NS094489, as well as by the Robert Wood Johnson Foundation, The Elsie and Marvin Dekelboum Family Foundation, the Liston Family Foundation, the Robert H. and Clarice Smith and Abigail van Buren Alzheimer's Disease Research Program, the Alexander Family Foundation, the GHR Foundation, Dr Corinne Schuler, and the Mayo Foundation for Medical Education and Research); Dr Seeley (funded by NIH grants P01AG019724 and P50AG023501 as well as by the Consortium for Frontotemporal Dementia Research and the Tau Consortium); Dr Ikonomovic (funded by NIH grants AG05133 and AG025204); and Dr Masdeu (funded by the Chao, Harrison, and Nantz Funds of the Houston Methodist Foundation).

Role of the Funder/Sponsor: The main funder, Avid Radiopharmaceuticals, had a role in the design and conduct of this study and the confirmatory reader study; collection, management, analysis, and interpretation of the data; preparation, review, and approval of the manuscript; and decision to submit the manuscript for publication. Avid Radiopharmaceuticals had no role in the original acquisition of the supplemental autopsy cases data, which were acquired, managed, and funded through independent collaborator protocols before transfer to Avid Radiopharmaceuticals.

Group Information: A16 Study Investigators: Murray Grossman, MD, EdD, University of Pennsylvania; Marc E. Agronin, MD, Miami Jewish Health; Alireza Atri, MD, PhD, Banner Sun Health Research Institute; Donald M. Brandon, MD, California Research Foundation; Richard S. Cherlin, MD, private practice; Robert C. Cupelo, MD, Clarity Clinical Research; Dagoberto de la Vega, MD, D de la Vega MD Research Group; Jamehl Demons Shegog, MD, Wake Forest School of Medicine; Kimiko Domoto-Reilly, MD, Memory and Brain Wellness Center, University of Washington; P. Murali Doraiswamy, MD, MBBS, Duke University School of Medicine; John G. Duffy, MD, MS, Syrentis Clinical Research; Jose E. Gamez, MD, BS, Galiz Research; Andrew W. Garner MD, Adirondack Medical Research Center; Allen J. Geltzer, MD, Radiant Clinical Research; William T. Hu, MD, PhD, Emory University School of Medicine; Cathy A. Hurley, MD, Sante Clinical Research; Gregory A. Kirk, MD, Merritt Island Medical Research, LLC; Colin L. Masters, MD, MBBS, The Florey Institute of Neuroscience and Mental Health; Anil K. Nair, MD, Alzheimer's Disease Center; Esteban Olivera, MD, MS, Bioclinica Research (formerly Compass Research); Jorg J. Pahl, MD, American Clinical Trials; Meenakshi C. Patel, MD, Valley Medical Research; Marvin L. Peyton, MD, Rivus Wellness and Research Institute; Frederick W. Schaerf, MD, PhD, Neuropsychiatric Research Center of Southwest Florida; William R. Shankle, MD, MS, The Shankle Clinic; Jiong Shi, MD, PhD, St Joseph's Hospital and Medical Center; Upinder Singh, MD, MBBS, Geriatric Solutions, LLC; Kaycee M. Sink, MD, MAS, Wake Forest School of Medicine; Stephen G. Thein; PhD, MA, Pacific Research Network, Inc.

REFERENCES

1. Goedert M, Jakes R. Mutations causing neurodegenerative tauopathies. *Biochim Biophys Acta*. 2005;1739(2-3):240-250. doi:10.1016/j.bbadis.2004.08.007

2. Kidd M. Paired helical filaments in electron microscopy of Alzheimer's disease. *Nature*. 1963;197:192-193. doi:10.1038/197192b0

3. Masters CL, Multhaup G, Simms G, Pottgiesser J, Martins RN, Beyreuther K. Neuronal origin of a cerebral amyloid: neurofibrillary tangles of Alzheimer's disease contain the same protein as the amyloid of plaque cores and blood vessels. *EMBO J*. 1985;4(11):2757-2763. doi:10.1002/j.1460-2075.1985.tb04000.x

4. Hyman BT. The neuropathological diagnosis of Alzheimer's disease: clinical-pathological studies. *Neurobiol Aging*. 1997;18(4)(suppl):S27-S32. doi:10.1016/S0197-4580(97)00066-3

5. Hyman BT, Phelps CH, Beach TG, et al. National Institute on Aging-Alzheimer's Association guidelines for the neuropathologic assessment of Alzheimer's disease. *Alzheimers Dement*. 2012;8(1):1-13. doi:10.1016/j.jalz.2011.10.007

6. Jack CR Jr, Bennett DA, Blennow K, et al; Contributors. NIA-AA research framework: toward a biological definition of Alzheimer's disease. *Alzheimers Dement*. 2018;14(4):535-562. doi:10.1016/j.jalz.2018.02.018

7. Dubois B, Feldman HH, Jacova C, et al. Revising the definition of Alzheimer's disease: a new lexicon. *Lancet Neurol*. 2010;9(11):1118-1127. doi:10.1016/S1474-4422(10)70223-4

8. McKhann GM, Knopman DS, Chertkow H, et al. The diagnosis of dementia due to Alzheimer's disease: recommendations from the National Institute on Aging-Alzheimer's Association workgroups on diagnostic guidelines for Alzheimer's disease. *Alzheimers Dement*. 2011;7(3):263-269. doi:10.1016/j.jalz.2011.03.005

9. Knopman DS, Petersen RC, Jack CR Jr. A brief history of "Alzheimer disease": multiple meanings separated by a common name. *Neurology*. 2019;92(22):1053-1059. doi:10.1212/WNL.0000000000007583

10. Avila J, Lucas JJ, Perez M, Hernandez F. Role of tau protein in both physiological and pathological conditions. *Physiol Rev*. 2004;84(2):361-384. doi:10.1152/physrev.00024.2003

11. Querfurth HW, LaFerla FM. Alzheimer's disease. *N Engl J Med*. 2010;362(4):329-344. doi:10.1056/NEJMra0909142

12. Dickson TC, Saunders HL, Vickers JC. Relationship between apolipoprotein E and the amyloid deposits and dystrophic neurites of Alzheimer's disease. *Neuropathol Appl Neurobiol*. 1997;23(6):483-491. doi:10.1111/j.1365-2990.1997.tb01325.x

13. Duyckaerts C, Brion JP, Hauw JJ, Flament-Durand J. Quantitative assessment of the density of neurofibrillary tangles and senile plaques in senile dementia of the Alzheimer type. Comparison of immunocytochemistry with a specific antibody and Bodian's protargol method. *Acta Neuropathol*. 1987;73(2):167-170. doi:10.1007/BF00693783

14. Nelson PT, Alafuzoff I, Bigio EH, et al. Correlation of Alzheimer disease neuropathologic changes with cognitive status: a review of the literature. *J Neuropathol Exp Neurol*. 2012;71(5):362-381. doi:10.1097/NEN.0b013e31825018f7

15. Wong DF, Rosenberg PB, Zhou Y, et al. In vivo imaging of amyloid deposition in Alzheimer disease using the radioligand 18F-AV-45 (florbetapir [corrected] F 18). *J Nucl Med*. 2010;51(6):913-920. doi:10.2967/jnumed.109.069088

16. Clark CM, Pontecorvo MJ, Beach TG, et al; AV-45-A16 Study Group. Cerebral PET with florbetapir compared with neuropathology at autopsy for detection of neuritic amyloid-β plaques: a prospective cohort study. *Lancet Neurol*. 2012;11(8):669-678. doi:10.1016/S1474-4422(12)70142-4

17. Curtis C, Gamez JE, Singh U, et al. Phase 3 trial of flutemetamol labeled with radioactive fluorine 18 imaging and neuritic plaque density. *JAMA Neurol*. 2015;72(3):287-294. doi:10.1001/jamaneurol.2014.4144

18. Sabri O, Sabbagh MN, Seibyl J, et al; Florbetaben Phase 3 Study Group. Florbetaben PET imaging to detect amyloid beta plaques in Alzheimer's disease: phase 3 study. *Alzheimers Dement*. 2015;11(8):964-974. doi:10.1016/j.jalz.2015.02.004

19. Chien DT, Bahri S, Szardenings AK, et al. Early clinical PET imaging results with the novel PHF-tau radioligand [F-18]-T807. *J Alzheimers Dis*. 2013;34(2):457-468. doi:10.3233/JAD-122059

20. Xia CF, Arteaga J, Chen G, et al. [(18)F]T807, a novel tau positron emission tomography imaging agent for Alzheimer's disease. *Alzheimers Dement*. 2013;9(6):666-676. doi:10.1016/j.jalz.2012.11.008

21. Pontecorvo MJ, Fleisher AS, Devous MD, et al. Baseline tau accumulation, as evidenced by visual interpretation of flortaucipir PET, and longitudinal cognitive change in three trials with MCI and AD dementia subjects. Paper presented at: 14th International Conference on Alzheimer's & Parkinson's Diseases; March 27, 2019; Lisbon, Portugal.

22. Southekal S, Devous MD Sr, Kennedy I, et al. Flortaucipir F 18 quantitation using parametric estimation of reference signal intensity. *J Nucl Med*. 2018;59(6):944-951. doi:10.2967/jnumed.117.200006

23. Pontecorvo MJ, Devous MD Sr, Navitsky M, et al; 18F-AV-1451-A05 investigators. Relationships between flortaucipir PET tau binding and amyloid burden, clinical diagnosis, age and cognition. *Brain*. 2017;140(3):748-763. doi:10.1093/brain/aww334

24. Devous MD Sr, Joshi AD, Navitsky M, et al. Test-retest reproducibility for the tau PET imaging agent flortaucipir F 18. *J Nucl Med*. 2018;59(6):937-943. doi:10.2967/jnumed.117.200691

25. Lowe VJ, Lundt ES, Albertson SM, et al. Tau-positron emission tomography correlates with neuropathology findings. *Alzheimers Dement*. 2020;16(3):561-571. doi:10.1016/j.jalz.2019.09.079

26. Josephs KA, Whitwell JL, Tacik P, et al. [18F]AV-1451 tau-PET uptake does correlate with quantitatively measured 4R-tau burden in autopsy-confirmed corticobasal degeneration. *Acta Neuropathol*. 2016;132(6):931-933. doi:10.1007/s00401-016-1618-1

27. Marquié M, Normandin MD, Meltzer AC, et al. Pathological correlations of [F-18]-AV-1451 imaging in non-Alzheimer tauopathies. *Ann Neurol*. 2017;81(1):117-128. doi:10.1002/ana.24844

28. Marquié M, Verwer EE, Meltzer AC, et al. Lessons learned about [F-18]-AV-1451 off-target binding from an autopsy-confirmed Parkinson's case. *Acta Neuropathol Commun*. 2017;5(1):75. doi:10.1186/s40478-017-0482-0

29. McMillan CT, Irwin DJ, Nasrallah I, et al. Multimodal evaluation demonstrates in vivo ^{18}F-AV-1451 uptake in autopsy-confirmed corticobasal degeneration. *Acta Neuropathol*. 2016;132(6):935-937. doi:10.1007/s00401-016-1640-3

30. Smith R, Puschmann A, Schöll M, et al. 18F-AV-1451 tau PET imaging correlates strongly with tau neuropathology in MAPT mutation carriers. *Brain*. 2016;139(pt 9):2372-2379. doi:10.1093/brain/aww163

31. Smith R, Schöll M, Honer M, Nilsson CF, Englund E, Hansson O. Tau neuropathology correlates with FDG-PET, but not AV-1451-PET, in progressive supranuclear palsy. *Acta Neuropathol*. 2017;133(1):149-151. doi:10.1007/s00401-016-1650-1

32. Day GS, Gordon BA, Perrin RJ, et al. In vivo [^{18}F]-AV-1451 tau-PET imaging in sporadic Creutzfeldt-Jakob disease. *Neurology*. 2018;90(10):e896-e906. doi:10.1212/WNL.0000000000005064

33. Smith R, Wibom M, Pawlik D, Englund E, Hansson O. Correlation of in vivo [18F]flortaucipir with postmortem Alzheimer disease tau pathology. *JAMA Neurol*. 2019;76(3):310-317. doi:10.1001/jamaneurol.2018.3692

34. Braak H, Alafuzoff I, Arzberger T, Kretzschmar H, Del Tredici K. Staging of Alzheimer disease-associated neurofibrillary pathology using paraffin sections and immunocytochemistry. *Acta Neuropathol*. 2006;112(4):389-404. doi:10.1007/s00401-006-0127-z

35. World Medical Association. World Medical Association Declaration of Helsinki: ethical principles for medical research involving human subjects. *JAMA*. 2013;310(20):2191-2194. doi:10.1001/jama.2013.281053

36. Dixon JR Jr. The International Conference on Harmonization Good Clinical Practice guideline. *Qual Assur*. 1998;6(2):65-74. doi:10.1080/105294199277860

37. Jorm AF. A short form of the Informant Questionnaire on Cognitive Decline in the Elderly (IQCODE): development and cross-validation. *Psychol Med*. 1994;24(1):145-153. doi:10.1017/S003329170002691X

38. Folstein MF, Folstein SE, McHugh PR. "Mini-mental state". A practical method for grading the cognitive state of patients for the clinician. *J Psychiatr Res*. 1975;12(3):189-198. doi:10.1016/0022-3956(75)90026-6

39. Abdi H, Williams LJ, Beaton D, et al. Analysis of regional cerebral blood flow data to discriminate among Alzheimer's disease, frontotemporal dementia, and elderly controls: a multi-block barycentric discriminant analysis (MUBADA) methodology. *J Alzheimers Dis*. 2012;31(suppl 3):S189-S201. doi:10.3233/JAD-2012-112111

40. Montine TJ, Phelps CH, Beach TG, et al; National Institute on Aging; Alzheimer's Association. National Institute on Aging-Alzheimer's Association guidelines for the neuropathologic assessment of Alzheimer's disease: a practical approach. *Acta Neuropathol*. 2012;123(1):1-11. doi:10.1007/s00401-011-0910-3

41. Thal DR, Rüb U, Orantes M, Braak H. Phases of A beta-deposition in the human brain and its relevance for the development of AD. *Neurology*. 2002;58(12):1791-1800. doi:10.1212/WNL.58.12.1791

42. Mirra SS, Heyman A, McKeel D, et al. The Consortium to Establish a Registry for Alzheimer's Disease (CERAD). Part II. Standardization of the neuropathologic assessment of Alzheimer's disease. *Neurology*. 1991;41(4):479-486. doi:10.1212/WNL.41.4.479

43. Mungas D, Tractenberg R, Schneider JA, Crane PK, Bennett DA. A 2-process model for neuropathology of Alzheimer's disease. *Neurobiol Aging*. 2014;35(2):301-308. doi:10.1016/j.neurobiolaging.2013.08.007

44. Monsell SE, Mock C, Roe CM, et al. Comparison of symptomatic and asymptomatic persons with Alzheimer disease neuropathology. *Neurology*. 2013;80(23):2121-2129. doi:10.1212/WNL.0b013e318295d7a1

45. Johnson KA, Schultz A, Betensky RA, et al. Tau positron emission tomographic imaging in aging and early Alzheimer disease. *Ann Neurol*. 2016;79(1):110-119. doi:10.1002/ana.24546

46. Nelson PT, Abner EL, Schmitt FA, et al. Brains with medial temporal lobe neurofibrillary tangles but no neuritic amyloid plaques are a diagnostic dilemma but may have pathogenetic aspects distinct from Alzheimer disease. *J Neuropathol Exp Neurol*. 2009;68(7):774-784. doi:10.1097/NEN.0b013e3181aacbe9

47. Jellinger KA, Alafuzoff I, Attems J, et al. PART, a distinct tauopathy, different from classical sporadic Alzheimer disease. *Acta Neuropathol*. 2015;129(5):757-762. doi:10.1007/s00401-015-1407-2

48. Bennett DA, Schneider JA, Wilson RS, Bienias JL, Arnold SE. Neurofibrillary tangles mediate the association of amyloid load with clinical Alzheimer disease and level of cognitive function. *Arch Neurol*. 2004;61(3):378-384. doi:10.1001/archneur.61.3.378

49. Bennett DA, Schneider JA, Bienias JL, Evans DA, Wilson RS. Mild cognitive impairment is related to Alzheimer disease pathology and cerebral infarctions. *Neurology*. 2005;64(5):834-841. doi:10.1212/01.WNL.0000152982.47274.9E

50. Ossenkoppele R, Rabinovici GD, Smith R, et al. Discriminative accuracy of [18F]flortaucipir positron emission tomography for Alzheimer disease vs other neurodegenerative disorders. *JAMA*. 2018;320(11):1151-1162. doi:10.1001/jama.2018.12917

51. Pontecorvo MJ, Devous MD, Kennedy I, et al. A multicentre longitudinal study of flortaucipir (18F) in normal ageing, mild cognitive impairment and Alzheimer's disease dementia. *Brain*. 2019;142(6):1723-1735. doi:10.1093/brain/awz090

52. Fleisher AS, Pontecorvo MJ, Devous MD, et al. Tau PET imaging as a screening tool for clinical trials of disease modifying therapies. *J Prev Alzheimers Dis*. 2018;5(S1):S17.

53. Siderowf AD, Keene CD, Beach TG, et al. Comparison of regional flortaucipir PET to quantitative tau and amyloid immunoassay in patients with Alzheimer's disease pathology: a pilot clinico-pathological study. *Alzheimers Dement*. 2017;13(7):776. doi:10.1016/j.jalz.2017.06.1038

54. Southekal S, Kotari V, Devous MD Sr, et al. Temporal lobe quantitation of flortaucipir PET images may improve detection of intermediate neurofibrillary tangle pathology in autopsy-validated cases. *Alzheimers Dement*. 2019;15(7):P1486-P1487. doi:10.1016/j.jalz.2019.08.008

55. Kotari V, Navitsky M, Southekal S, et al. Early tau detection and implications for disease progression. *Alzheimers Dement*. 2019;15(7):P1614-P1615. doi:10.1016/j.jalz.2019.06.4839

56. Dickstein DL, Pullman MY, Fernandez C, et al. Cerebral [^{18} F]T807/AV1451 retention pattern in clinically probable CTE resembles pathognomonic distribution of CTE tauopathy. *Transl Psychiatry*. 2016;6(9):e900. doi:10.1038/tp.2016.175

57. Schonhaut DR, McMillan CT, Spina S, et al. ^{18} F-flortaucipir tau positron emission tomography distinguishes established progressive supranuclear palsy from controls and Parkinson disease: a multicenter study. *Ann Neurol*. 2017;82(4):622-634. doi:10.1002/ana.25060